



Direct extrusion of thin Mg wires for biomedical applications

K. TESAŘ^{1,2}, K. BALÍK³, Z. SUCHARDA³, A. JÄGER⁴

1. Department of Materials, Faculty of Nuclear Sciences and Physical Engineering, Czech Technical University in Prague, Trojanova 13, Prague, 120 00, Czech Republic;
2. Department of Dielectrics, Institute of Physics, Czech Academy of Sciences, Na Slovance 2, Prague, 182 21, Czech Republic;
3. Department of Composites and Carbon Materials, Institute of Rock Structure and Mechanics, Czech Academy of Sciences, V Holešovičkách 41, Prague, 182 09, Czech Republic;
4. Department of Mechanics, Faculty of Civil Engineering, Czech Technical University in Prague, Thákurova 7, Prague, 166 29, Czech Republic

Received 17 April 2019; accepted 11 November 2019

Abstract: Biodegradable wires, able to provide load-bearing support for various biomedical applications, are the novel trends in current biomaterial research. A thin 99.92% Mg wire with a diameter of 250 μm was prepared via direct extrusion with an extreme reduction ratio of 1:576. The total imposed strain in a single processing step was 6.36. Extrusion was carried out at elevated temperatures in the range from 230 to 310 $^{\circ}\text{C}$ and with various ram speeds ranging from ~ 0.2 to ~ 0.5 mm/s. The resulting wires show very good mechanical properties which vary with extrusion parameters. Maximum true tensile stress at room temperature reaches ~ 228 MPa and ductility reaches $\sim 13\%$. The proposed single-step direct extrusion can be an effective method for the production of Mg wires in sufficient quantities for bioapplications. The fractographic analysis revealed that failure of the wires may be closely connected with inclusions (e.g., MgO particles). The results are essential for determining the optimal processing conditions of hot extrusion for thin Mg wire. The smaller grain size, as the outcome of the lower extrusion temperature, is identified as the main parameter affecting the tensile properties of the wires.

Key words: biomedical materials; mechanical properties; fracture; nonferrous metals; magnesium

1 Introduction

Pure magnesium is principally very promising material due to its low density, reasonable specific strength and biodegradability in the human body. Inferior mechanical properties of this material are commonly overcome by alloying which allow the optimization for various applications, such as structural and biomedical [1]. Well-known property of pure magnesium is biodegradability [1]. This attribute can be employed in various ways. Since the magnesium has similar elastic modulus as bone tissue, it is an exceptional and biocompatible

material for various implants [2]. These implants are gradually replaced by human cells due to the biodegradability of magnesium and the fact that magnesium supports tissue regeneration [1,3]. Various porous forms of magnesium are used to further enhance this effect [4]. In terms of tuning biodegradable properties of pure Mg, the most viable elements are rare earth Y, Gd and Nd due to precipitation hardening and their reasonable biocompatibility [5–7]. Other widely used systems are Mg–Zn [8], Mg–Ca [9] and Mg–Zn–Al [10]. However, alloying elements may introduce additional problems in terms of biocompatibility and formability when considering very thin wires.

Therefore, it can be beneficial to use pure magnesium.

To obtain the required mechanical properties without the addition of alloying elements, it is necessary to employ techniques which reduce grain size or create a strong preferential orientation of grains (i.e., texture). Among these, severe plastic deformation techniques, such as equal channel angular pressing (ECAP) [11,12] and high-pressure torsion (HPT) [13], have been frequently used. However, they are limited by low productivity. Another way to reduce grain size to the desired level would be expanding the limits of high-productivity forming techniques such as direct extrusion [14]. The advanced design of the extrusion dies, together with recent progress in the development of high strength steels, has enabled to transform the conventional forming process into an efficient production method of thin Mg wires.

In recent years, significant attention has been paid to the possible application of thin Mg wires for stents and suture material [15] or as a support for phosphate cement or biodegradable polymers, used for bone replacements and fracture fixation devices [16,17]. For these applications, it is necessary to obtain Mg with high strength, while maximizing ductility, which is typically inferior for alloyed wires produced by cold drawing technique [18]. The main disadvantage of cold drawing is the number of processing steps to obtain small wire diameters. It is also necessary to anneal the material between subsequent cold drawing steps which is very time consuming and thus a costly process of Mg wire production [19].

Pure magnesium wires with very good mechanical properties could be used in a large number of applications, ranging from the suture material and bone support to the biodegradable composite reinforcement. For the purpose of magnesium bioabsorbable wire product development, we extruded Mg wire with a diameter of 250 μm . This was achieved by single-pass extrusion of a pure Mg billet with an initial diameter of 6 mm via extrusion die with extreme reduction ratio. In this work, we discuss the resulting mechanical properties and microstructure of the material with respect to the different processing parameters. This work determines the ideal processing parameters for this material and serves as a starting point for future research of

wires intended for sternal fixation and other bone support medical applications.

2 Experimental

The composition of the initial material, as measured by glow discharge optical emission spectrometry (GDOES), using the spectrometer Spectruma GDA HR 750, is listed in Table 1. For these measurements, a large number of certified reference materials were used to obtain reliable results.

Table 1 Chemical composition of pure Mg block as measured by GDOES (wt.%)

Zn	O	Cu	Al	Fe	Mg
0.04	0.02	0.006	0.004	0.003	Bal.

Electro-discharge machining (EDM) was used to cut cylindrical specimens with dimensions of $d6 \text{ mm} \times 18 \text{ mm}$ from the block of pure Mg. These specimens were then cleaned in a 10% aqueous solution of HNO_3 to remove EDM residue and subjected to a direct extrusion process with the exit channel diameter of 250 μm . The scheme of the direct extrusion die with the relevant coordinate system is shown in Fig. 1, where ED and RD denote extrusion and radial direction, respectively. The resulting extrusion ratio for this die geometry equals 1:576. Processing was carried out at elevated temperatures in the range from 230 to 310 $^\circ\text{C}$ and at various ram speeds, from 0.2 to 0.5 mm/s. The wire was subsequently coiled on a $d100 \text{ mm}$ reel.

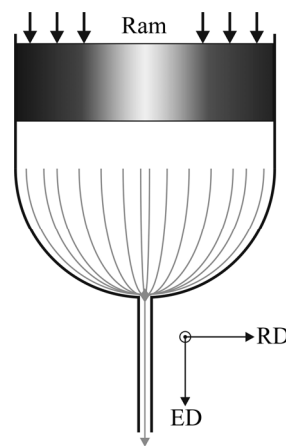


Fig. 1 Scheme of direct extrusion die channel with coordinate system for reference (ED—Extrusion direction; RD—Radial direction)

Magnesium wires with the gauge length of 30 mm were deformed on the Instron 5882 testing machine with 100 N load cell at room temperature (RT). Pneumatic grips for wire testing were used. The number of measurements for each ram speed was 3–8 to obtain statistically relevant data set. Additional tests were conducted to characterize the strain rate sensitivity of the extruded wires, with initial strain rates in the range from 10^{-4} to 10^{-1} s^{-1} .

For the purpose of microstructural analysis of the as-cast magnesium, a light microscope AxioObserver D1m was used. Sample preparation consisted of cold-mounting the specimens in an epoxy resin (Struers EpoFix), plane grinding with progressively finer SiC papers and mechanical polishing with diamond suspensions of particle sizes of 3 and 1 μm . Final polishing was performed with a solution of colloidal silica (Struers OP-S). In some cases, a 3% nital (solution of nitric acid in ethanol) was used to provide additional grain boundary and phase contrast. A routine examination of the grain size of the as-extruded wires was performed by etching the wire surface in 5% solution of nitric acid in distilled water for 20 s. The

surface topography of these etched wires was observed with scanning electron microscope FEI Phenom. A scanning electron microscope FEI Quanta 3D FEG was used for the fractographic analysis and energy dispersive spectrometry (EDS). For estimating the average grain size, a linear intercept method on at least three SEM micrographs was used with a total line length of 1000 μm : 500 μm in the ED and 500 μm in the RD. Since the grains were equiaxed for all wires, one average grain size was reported for each wire. Resulting average intercept length was multiplied by a factor of 1.57 to obtain average grain size [20].

3 Results and discussion

3.1 Tensile properties

Magnesium wires were extruded at different ram speeds and temperatures. Subsequently, the wires were deformed in tension at the initial strain rate of $1 \times 10^{-3} \text{ s}^{-1}$. The results listed in Table 2 show that higher values of characteristic stresses $\sigma_{0.2}$, σ_{max} and elongation to failure A correspond with the lower temperature of extrusion and vice versa.

Table 2 Mechanical properties of Mg wires in respect to processing temperature and ram speed

Extrusion temperature/ $^{\circ}\text{C}$	Ram speed/ $(\text{mm} \cdot \text{s}^{-1})$	$\sigma_{0.2}/\text{MPa}$	$\sigma_{\text{max}}/\text{MPa}$	$A/\%$	Number of tensile samples
230	0.2	136 \pm 4	228 \pm 1	13.7 \pm 0.1	3
	0.4	132 \pm 3	219 \pm 1	13.5 \pm 1.8	4
240	0.2	127 \pm 3	218 \pm 2	11.7 \pm 1.0	4
	0.2	122 \pm 4	223 \pm 4	12.3 \pm 0.6	5
250	0.3	124 \pm 3	221 \pm 5	11.5 \pm 1.7	5
	0.4	130 \pm 3	227 \pm 3	13.4 \pm 0.1	4
260	0.2	123 \pm 3	222 \pm 3	11.6 \pm 1.0	9
	0.3	121 \pm 4	225 \pm 1	10.3 \pm 0.6	5
	0.4	118 \pm 3	215 \pm 5	12.7 \pm 1.3	4
	0.5	118 \pm 4	217 \pm 1	12.5 \pm 0.8	4
270	0.2	115 \pm 4	219 \pm 9	9.9 \pm 1.0	6
	0.3	120 \pm 3	222 \pm 2	11.1 \pm 0.1	3
	0.4	118 \pm 2	221 \pm 3	11.0 \pm 1.1	4
290	0.5	118 \pm 4	209 \pm 9	8.0 \pm 0.8	5
	0.2	111 \pm 5	217 \pm 4	10.1 \pm 0.4	9
300	0.2	101 \pm 4	208 \pm 3	10.1 \pm 0.8	6
	0.3	106 \pm 1	220 \pm 2	11.5 \pm 1.0	5
	0.4	101 \pm 1	204 \pm 2	10.3 \pm 0.8	4
	0.5	107 \pm 2	214 \pm 1	9.5 \pm 0.3	4
310	0.2	104 \pm 2	215 \pm 2	8.9 \pm 0.5	6

$\sigma_{0.2}$ —Yield strength; σ_{max} —Maximum true tensile strength; A —Ductility

On the other hand, mechanical properties of the wires extruded at all temperatures are sufficient for many applications. From the data presented in Table 2, it is also apparent that the ram speed has only a minor effect on tensile properties. The ram speed can be maximized with respect to the strength limit of the extrusion die and plunger to produce the wires effectively and economically. It is important to mention that for such large reduction ratio and lower extrusion temperatures (230–260 °C) for pure Mg, the peak load on the press plunger can reach ~2 GPa. Nevertheless, if the presence of the inclusions in Mg ingot is controlled, the common value of the load on the press plunger at 300 °C reaches 880 MPa. The mechanical limit for extrusion die and plunger used in this work is ~2.2 GPa.

The best results of maximal true stress and ductility were achieved for the lowest extrusion temperature of 230 °C and low ram speed of 0.2 mm/s. High maximal true stress for this temperature is caused by lower activity of thermally activated phenomena triggering softening processes such as dynamic recovery, recrystallization and grain growth [18]. Processing temperature below 230 °C has caused problems with braking of the wire during the extrusion process.

Curves in Fig. 2 present the dependence of the tensile properties on the initial strain rate $\dot{\epsilon}$. Values of $\sigma_{0.2}$ and σ_{\max} decrease with decreasing initial strain rate and the dependence shows nearly linear course in semi-logarithmic scale (Fig. 2(a)). The main mechanism responsible for the changes in mechanical properties with strain rate can be connected with thermally activated dynamic recovery, easily taking place in very pure Mg even at room temperature and causing an observable dependence. At lower strain rates, dynamic recovery provides more time for relaxation of internal stresses. This lowers both values of characteristic stresses with decreasing strain rate. The resulting higher triaxiality of deformation promotes easier activation of additional slip systems and thus lowers the $\sigma_{0.2}$ and σ_{\max} [21].

The results also show that the ductility at a relatively fast strain rate of $1 \times 10^{-1} \text{ s}^{-1}$ is approximately 8% which is still good value for this material, sample geometry and dimensions (Fig. 2(b)). Error bars in Fig. 2 do not exceed 5% of the mean value for each data point and therefore are not presented in the graphs.

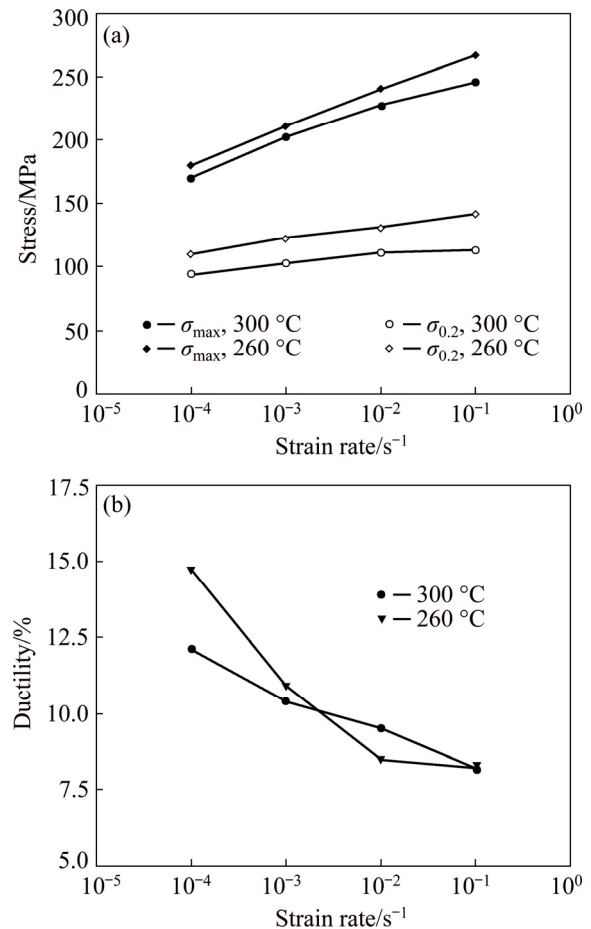


Fig. 2 Mechanical properties of Mg wires with respect to initial strain rate for two extrusion temperatures (260 and 300 °C): (a) $\sigma_{0.2}$ and σ_{\max} ; (b) Ductility

The obtained results of mechanical properties are interesting for biomedical applications. In this work, we produced 250 μm wires, which could be potentially used for fixation wires after median sternotomy in pediatrics. The physiologic loads on human sternum are commonly considered less than 400 N for an adult [22]. Ideally, we would design the wires to easily withstand 400 N load without the change of shape, under the yield strength. For that, we would need (for wires prepared at 230 °C, $\sigma_{0.2} \approx 130 \text{ MPa}$) no less than 63 wires. For single wires, this is clearly not achievable. However, usage of Mg wires with larger diameter could have a negative impact on the exceptional bending plasticity of these wires, as discussed by JÄGER et al [14]. Commonly, the sternal wires have diameter larger than 700 μm . Therefore, it would be beneficial to create at least 6-strand rope out of the 250 μm wire produced in this work. The diameter of this rope would be comparable to the ordinary

used wires and the presence of more wires supporting each site should significantly decrease the risk of failure during the biodegradation. It is clear that even when using 6-strand rope at a total of 6–8 sites, the wires do not achieve the required load-bearing capacity for an adult. However, the physiologic loads are significantly lower for children and infants, where the benefit of biodegradable sternal wires would be much higher. Apart from the usage of Mg wire ropes, careful biomechanical experiments and modeling are therefore still required to set the limits, where the Mg wire can be used from the mechanical point of view.

Another promising application would be biodegradable stents. For this, the wire diameter would ideally be even smaller [23]. The one-step method shown in this work is capable of producing Mg wires with diameter of 150 μm (at 300 $^{\circ}\text{C}$) without any problems. Furthermore, a 50 μm wire was also produced in limited quantities and quality, which is a current limit of the extrusion setup. In this work, we focus only on the 250 μm wire, intended mainly for sternal fixation.

3.2 Fractographic analysis

After the tensile testing at RT, selected samples with different ram speeds and extrusion temperature were subjected to fracture analysis in SEM. The observation of fracture surfaces revealed ductile behavior of the material and presence of particles in the microstructure (Fig. 3(a)). Figure 3(b) shows electron dispersive X-ray spectroscopy (EDS) of the particle in Fig. 3(a). EDS analysis conducted on several particles identified their composition as MgO.

It is worth mentioning that the majority of fracture surfaces inspected after the tensile tests contained these MgO particles. These particles most likely originate from insufficient atmosphere control during Mg casting process [24]. Presence of these particles has a detrimental influence on the mechanical properties of thin Mg wires because their size is not negligible compared to the wire diameter. It is therefore necessary to carefully control metallurgical processes and prevent the formation of these particles.

Figure 4 shows the fracture surfaces which were taken in two planes: the first approximately parallel with ED and the latter perpendicular to ED.

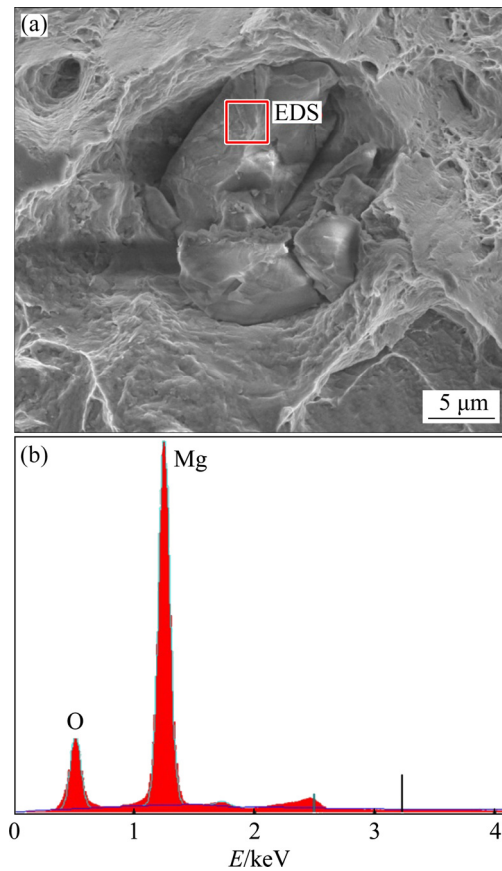


Fig. 3 SEM image of large MgO particles on fracture surface (a) and EDS spectrum of observed particle (b)

The extrusion temperature of Mg wires seems to have an influence on the overall profile of the fracture surface and associated morphology of the ductile dimples. For samples extruded at lower temperature (230 $^{\circ}\text{C}$), the fracture profile of the wire cross-section resembled a truncated cone (Fig. 4(a)). Thus, in the middle part of the cross-section, the equiaxed dimples were observed (Fig. 4(a)). In contrast, samples extruded at higher temperature (>290 $^{\circ}\text{C}$) were sheared through the whole cross-section and the dimples were rather deformed and elongated (Fig. 4(b)). Moreover, ductile dimples were not observed on the circumference areas of the cross-section due to the large amount of local shearing which indicates the activation of slip systems with higher critical resolved shear stress [21].

3.3 Microstructure

In order to explain differences in the mechanical properties of the wires processed under various conditions, microstructural characterization was performed. The initial microstructure of the

as-cast Mg ingot is composed of equiaxed grains with sizes varying from hundreds of micrometers up to centimeters (Fig. 5(a)). An occasional presence of other phases, identified as MgO by EDS, was also detected in the as-cast ingot. Figures 5(b, c) show the presence of MgO clusters identified as possible stress concentrators which initiate fracture in Mg wires during tensile testing (Fig. 3). Figure 5(b) shows a detail of MgO cluster with approximately circular shape and a larger MgO particle present in the upper right corner of the micrograph. Figure 5(c) shows a detail of a group of MgO particles surrounded by fine dispersion. It is rather difficult to remove oxide particles from the Mg ingot since they cannot be removed by melt settling [24].

Apart from the aforementioned initiation of the fracture process, larger particles could also cause geometrical irregularities of the wire cross-section.

A typical defect of the wire circularity is depicted by a white arrow in Fig. 5(d). Defects of this type are generally caused by three possible reasons: (1) The extrusion channel was damaged and a part of the die material partially blocked the extrusion channel; (2) Part of the 250 μm extrusion channel was blocked by MgO particle; (3) The channel is blocked by a foreign particle contained in lubricant or present in the extrusion channel from previous processing step. Another common defect of the hot-extruded wire is a diameter variance along the wire. This can be avoided by inspecting the wire diameter and reconditioning the extrusion die when the wire diameter variance is too large. For this purpose, the parts of the extrusion die, where the actual extrusion takes place, should be easily replaceable.

Despite the presence of oxide inclusions, the standard deviation of mechanical properties is very

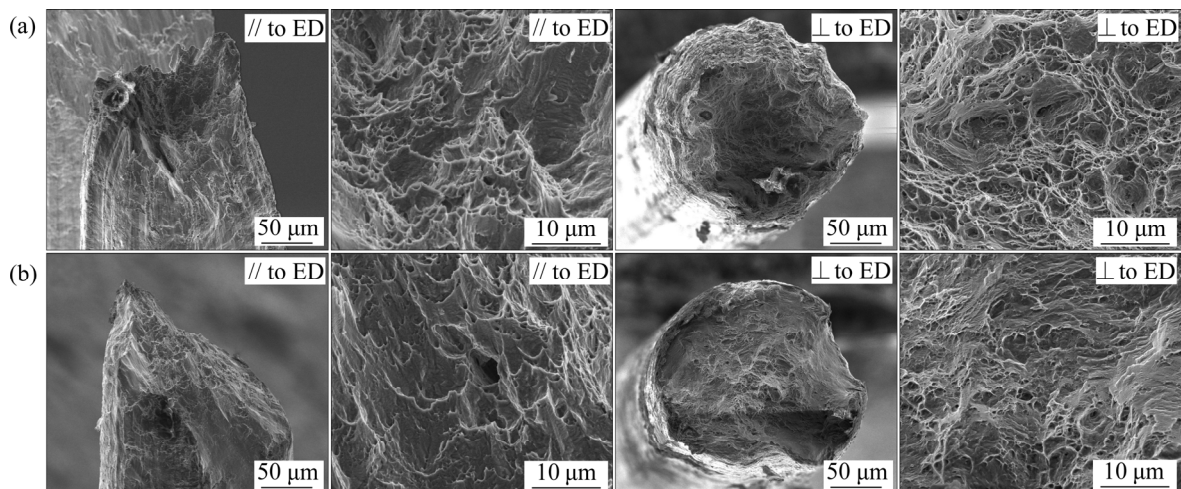


Fig. 4 Fracture surfaces of Mg wires after tensile test and details of ductile dimples from views approximately parallel (//) and perpendicular (\perp) to extrusion direction at different extrusion temperatures (strain rate $1 \times 10^{-3} \text{ s}^{-1}$): (a) 230 °C; (b) 300 °C

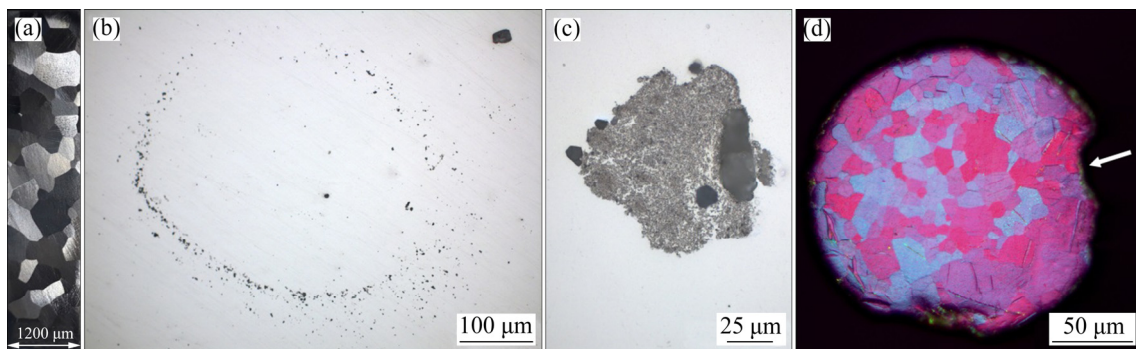


Fig. 5 Overview of microstructure of as-received Mg ingot (a), large cluster of MgO particles (b), detail of compact MgO cluster (c), and Mg wire cross-section (Arrow indicates irregularity of wire, possibly caused by MgO particle blocking die exit channel (polarized light)) (d)

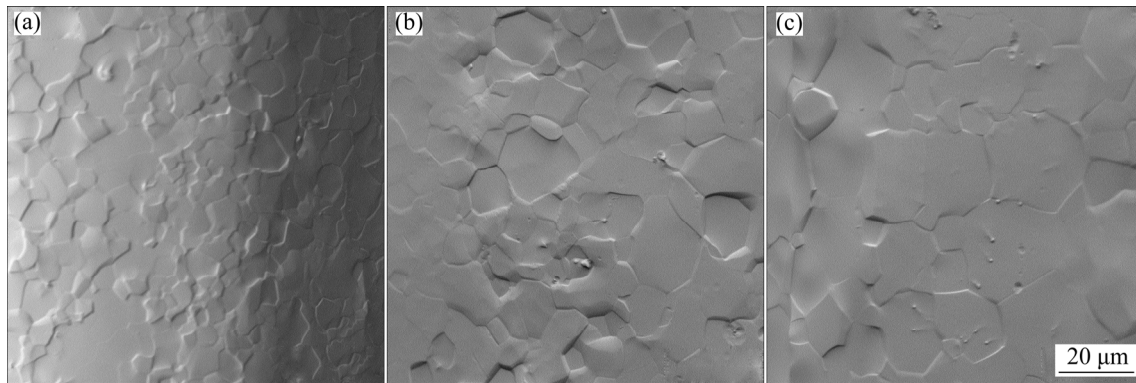


Fig. 6 SEM micrographs comparing grain size of Mg wires produced at different extrusion temperatures (ram speed is 0.2 mm/s for all wires): (a) 230 °C; (b) 260 °C; (c) 300 °C

small (Table 2). This may imply that MgO particles were distributed in each tensile test sample. With respect to the observed MgO on fracture surfaces, removing the MgO particles could improve the ductility. The presence of some twins on the perimeter of the wire (Fig. 5(d)) is likely connected with the mechanical preparation of the sample. On the other hand, bending of the wires produced reversible $\{10\bar{1}2\}$ mechanical twinning as an accommodating mechanism of plastic deformation [14]. Since twinning is a well-defined preparation artifact, it is possible to calculate grain size even when the twinning occurs.

In order to qualitatively compare differences in grain size for different extrusion temperatures, the wires were etched in 5% nitric acid and then studied by SEM. Figure 6 shows microstructures produced by extruding the wire at three different temperatures, namely 230, 260 and 300 °C. It can be seen that with increasing extrusion temperature, the resulting grain size is also increased. The average grain sizes for microstructures shown in Fig. 6 were 7, 11 and 14 μm for 230, 260 and 300 °C, respectively. This supports results in Table 2, where mechanical properties are best for the wire extruded at 230 °C as it approximately follows the Hall–Petch relationship [25,26]. On the other hand, the differences in the grain size were not noticeable for various ram speeds used in this work. Grain size of produced wires is quite large, considering the extrusion ratio that was used [27]. This is caused by the fact that the wires are exposed to elevated temperature during their reeling. Nevertheless, the resulting grain size is beneficial, as explained in detail in Ref. [14].

4 Conclusions

(1) Mechanical behavior of 99.92% magnesium wires with a diameter of 250 μm prepared by a single-step direct extrusion, with respect to the processing parameters and microstructure was analyzed. For the material processed at 230 °C, maximum tensile stress of (228 ± 1) MPa and corresponding ductility of $(13.7\pm 0.1)\%$ were obtained. Considering the purity of Mg matrix used, and effectiveness of the wire processing technique, this is an outstanding result.

(2) Fractographic analysis revealed the presence of MgO particles as a significant contributor to failure. High strain rate sensitivity of mechanical properties was attributed to the dynamic recovery which easily took place in very pure Mg and supported the development of necking at lower tensile strain rates. Triaxiality in necking in the case of lower strain rates facilitated activation of slip systems with higher critical resolved shear stress. This conclusion was further supported by the fractographic analysis of ductile dimples, present on the fracture surfaces.

(3) Different grain size of the as-extruded wire was the main reason for the different tensile properties achieved by lowering the extrusion temperature. These results are crucial for the ongoing development of biodegradable magnesium wires, finally intended for sternal wiring of infants and children, where current methods of non-degradable sternal fixation introduce the most severe complications.

Acknowledgments

Financial support of the Czech Technical University in Prague in the frame of the project SGS18/191/OHK4/3T/14 and financial support of the European Regional Development Fund (project CZ.02.1.01/0.0/0.0/16-019/0000778) are gratefully acknowledged. The authors would like to thank A. JANČOVÁ and M. KŘÍŽKOVÁ for technical assistance.

References

- [1] STAIGER M P, PIETAK A M, HUADMAI J, DIAS G. Magnesium and its alloys as orthopedic biomaterials: A review [J]. *Biomaterials*, 2006, 27: 1728–1734.
- [2] WITTE F. The history of biodegradable magnesium implants: A review [J]. *Acta Biomaterialia*, 2010, 6: 1680–1692.
- [3] LI Xia, LIU Xiang-mei, WU Shui-lin, YEUNG K W K, ZHENG Yu-feng, CHU P K. Design of magnesium alloys with controllable degradation for biomedical implants: From bulk to surface [J]. *Acta Biomaterialia*, 2016, 45: 2–30.
- [4] YAZDIMAMAGHANI M, RAZAVI M, VASHAEE D, MOHARAMZADEH K, BOCCACCINI A R, TAYEBI L. Porous magnesium-based scaffolds for tissue engineering [J]. *Materials Science and Engineering C*, 2017, 71: 1253–1266.
- [5] FARZADFAR S A, SANJARI M, JUNG I H, ESSADIQI E, YUE S. Role of yttrium in the microstructure and texture evolution of Mg [J]. *Materials Science and Engineering A*, 2011, 528: 6742–6753.
- [6] HORT N, HUANG Y, FECHNER D, STÖRMER M, BLAWERT C, WITTE F, VOGT C, DRÜCKER H, WILLUMEIT R, KAINER K U, FEYERABEND F. Magnesium alloys as implant materials – Principles of property design for Mg–RE alloys [J]. *Acta Biomaterialia*, 2010, 6: 1714–1725.
- [7] HADORN J P, AGNEW S R. A new metastable phase in dilute, hot-rolled Mg–Nd alloys [J]. *Materials Science and Engineering A*, 2012, 533: 9–16.
- [8] YAN Yang, CAO Han-wen, KANG Yi-jun, YU Kun, XIAO Tao, LUO Jie, DENG You-wen, FANG Hong-jie, XIONG Han-qing, DAI Yi-long. Effects of Zn concentration and heat treatment on the microstructure, mechanical properties and corrosion behavior of as-extruded Mg–Zn alloys produced by powder metallurgy [J]. *Journal of Alloys and Compounds*, 2017, 693: 1277–1289.
- [9] BIAN Dong, ZHOU Wei-wei, LIU Yang, LI Nan, ZHENG Yu-feng, SUN Zhi-li. Fatigue behaviors of HP-Mg, Mg–Ca and Mg–Zn–Ca biodegradable metals in air and simulated body fluid [J]. *Acta Biomaterialia*, 2016, 41: 351–360.
- [10] CHU C L, HAN X, BAI J, XUE F, CHU P K. Fabrication and degradation behavior of micro-arc oxidized biomedical magnesium alloy wires [J]. *Surface and Coatings Technology*, 2012, 213: 307–312.
- [11] JÄGER A, GÄRTNEROVÁ V, MUKAI T. Micro-mechanisms of grain refinement during extrusion of Mg–0.3at.%Al at low homologous temperature [J]. *Materials Characterization*, 2014, 93: 102–109.
- [12] JÄGER A, GÄRTNEROVÁ V, TESAŘ K. Microstructure and anisotropy of the mechanical properties in commercially pure titanium after equal channel angular pressing with back pressure at room temperature [J]. *Materials Science and Engineering A*, 2015, 644: 114–120.
- [13] ZHANG C Z, ZHU S J, WANG L G, GUO R M, YUE G C, GUAN S K. Microstructures and degradation mechanism in simulated body fluid of biomedical Mg–Zn–Ca alloy processed by high pressure torsion [J]. *Materials & Design*, 2016, 96: 54–62.
- [14] JÄGER A, HABR S, TESAŘ K. Twinning–detwinning assisted reversible plasticity in thin magnesium wires prepared by one-step direct extrusion [J]. *Materials & Design*, 2016, 110: 895–902.
- [15] BAI Jing, YIN Ling-ling, LU Ye, GAN Yi-wei, XUE Feng, CHU Cheng-lin, YAN Jing-li, YAN Kai, WAN Xiao-feng, TANG Zhe-jun. Preparation, microstructure and degradation performance of biomedical magnesium alloy fine wires [J]. *Progress in Natural Science: Materials International*, 2014, 24: 523–530.
- [16] KRÜGER R, SEITZ J M, EWALD A, BACH F W, GROLL J. Strong and tough magnesium wire reinforced phosphate cement composites for load-bearing bone replacement [J]. *Journal of the Mechanical Behavior of Biomedical Materials*, 2013, 20: 36–44.
- [17] WU Y H, LI N, CHENG Y, ZHENG Y F, HAN Y. In vitro study on biodegradable AZ31 magnesium alloy fibers reinforced PLGA composite [J]. *Journal of Materials Science & Technology*, 2013, 29: 545–550.
- [18] QIAO Yan-dang, WANG Xin, LIU Zu-yan, WANG Er-de. Microstructures, textures and mechanical properties evolution during cold drawing of pure Mg [J]. *Microscopy Research*, 2013, 1: 8–15.
- [19] CHAO H Y, SUN H F, CHEN W Z, WANG E D. Static recrystallization kinetics of a heavily cold drawn AZ31 magnesium alloy under annealing treatment [J]. *Materials Characterization*, 2011, 62: 312–320.
- [20] MENDELSON M I. Average grain size in polycrystalline ceramics [J]. *Journal of the American Ceramic Society*, 1969, 52: 443–446.
- [21] RODRIGUEZ A K, AYOUB G A, MANSOOR B, BENZERGA A A. Effect of strain rate and temperature on fracture of magnesium alloy AZ31B [J]. *Acta Materialia*, 2016, 112: 194–208.
- [22] MCGREGOR W E, TRUMBLE D R, MAGOVERN J A. Mechanical analysis of midline sternotomy wound closure [J]. *The Journal of Thoracic and Cardiovascular Surgery*, 1999, 117: 1144–1150.
- [23] ANG H Y, BULLUCK H, WONG P, VENKATRAMAN S S, HUANG Y Y, FOIN N. Bioresorbable stents: Current and upcoming bioresorbable technologies [J]. *International Journal of Cardiology*, 2017, 228: 931–939.
- [24] LUN SIN S, ELSAYED A, RAVINDRAN C. Inclusions in magnesium and its alloys: A review [J]. *International Materials Reviews*, 2013, 58: 419–436.
- [25] YUAN W, PANIGRAHI S K, SU J Q, MISHRA R S. Influence of grain size and texture on Hall–Petch relationship for a magnesium alloy [J]. *Scripta Materialia*, 2011, 65: 994–997.

- [26] SOMEKAWA H, MUKAI T. Hall–Petch relation for deformation twinning in solid solution magnesium alloys [J]. *Materials Science and Engineering A*, 2013, 561: 378–785.
- [27] SUN Hong-fei, LI Cheng-jie, XIE Yang, FANG Wen-bin. Microstructures and mechanical properties of pure magnesium bars by high ratio extrusion and its subsequent annealing treatment [J]. *Transactions of Nonferrous Metals Society of China*, 2012, 22(S): s445–s449.

直接挤压成形生物医用镁合金细丝

K. TESAŘ^{1,2}, K. BALÍK³, Z. SUCHARDA³, A. JÄGER⁴

1. Department of Materials, Faculty of Nuclear Sciences and Physical Engineering, Czech Technical University in Prague, Trojanova 13, Prague, 120 00, Czech Republic;

2. Department of Dielectrics, Institute of Physics, Czech Academy of Sciences, Na Slovance 2, Prague, 182 21, Czech Republic;

3. Department of Composites and Carbon Materials, Institute of Rock Structure and Mechanics, Czech Academy of Sciences, V Holešovičkách 41, Prague, 182 09, Czech Republic;

4. Department of Mechanics, Faculty of Civil Engineering, Czech Technical University in Prague, Thákurova 7, Prague, 166 29, Czech Republic

摘要: 生物可降解丝可为各种生物医学应用提供承重支撑, 是目前生物材料研究的新趋势。通过直接挤压制备出直径为 250 μm 的 99.92% 镁丝, 挤压比达 1:576。单个加工步骤的总施加应变为 6.36。挤压温度为 230~310 $^{\circ}\text{C}$, 挤压速度为 0.2~0.5 mm/s。得到的金属丝具有良好的力学性能, 其力学性能随挤压参数的变化而变化。室温下最大真拉应力可达 228 MPa, 塑性可达 13%。结果表明, 单步直接挤压法是一种有效的生产具有足够性能的生物医用镁丝的方法。断口分析表明, 镁丝的失效可能与夹杂物(如 MgO 颗粒)密切相关。由于挤压温度低而导致的晶粒尺寸细小, 是影响镁丝拉伸性能的主要参数。

关键词: 生物医用材料; 力学性能; 断裂; 有色金属; 镁

(Edited by Bing YANG)